Grain boundary planes and their energies as estimated by dihedral angle measurements in nickel

Valerie Randle

Department of Materials Engineering, University College, Swansea, SA2 8PP, U.K.

Abstract. — Grain misorientations and boundary plane orientations have been measured for a sample population of grain boundaries in nickel. $\Sigma = 3$ boundaries were widespread, and the majority of them were either symmetrical or asymmetrical tilts on the 011 zone. The dihedral angles at grain junctions have also been measured and correlated with the relative grain boundary energy. From these data it was inferred that asymmetrical tilt $\Sigma = 3$s are low energy, although the resolution of the dihedral angle technique was insufficient to distinguish a hierarchy of relative energies within the $\Sigma = 3$ tilt class. The applicability of the well-established dihedral angle approach to assessment of relative grain boundary energy is discussed, particularly in the light of modern scanning electron microscopy diffraction techniques. The advantages of electron backscatter diffraction in a scanning electron microscope compared to transmission electron microscopy for grain boundary studies in polycrystalline materials are also highlighted.

1. Introduction.

The properties of grain boundaries in polycrystals are governed principally by their crystallography. Furthermore, the connectivity of so-called 'special' boundaries is a factor in determining the overall properties of a material [1]. With the advent of experimental techniques such as electron back-scatter diffraction (EBSD) in a scaning electron microscope (SEM) [2, 3], measurement of grain boundary geometry and topology can be performed routinely on a large scale, which is often an advantage over transmission electron microscopy (TEM). The following are the major parameters which are currently being determined using EBSD and SEM:

1) Spatially specific grain orientations from which misorientations can be calculated;
2) Disclination characterisation of grain junctions (triple lines) [4, 5];
3) Crystallographic orientation of grain boundary surfaces (planes) [1, 6, 7];
4) Connectivity of the grain surface network in three dimensions [1, 8];
5) True dihedral angles at grain junctions [9].

Having accessed these crystallographic and topological parameters, the ultimate goal is to correlate them with particular grain boundary properties e.g. diffusivity, free energy. This presents far more experimental difficulties than does obtaining crystallographic and topological data. However, the distribution of dihedral angles at a grain junction line provides a straightforward way of

assessing relative boundary energies (see next section) and has been used in this way for many years, often utilising the fact that twin boundaries can be recognised from their morphology [10, 11]. The present paper revisits the dihedral angle approach to assessment of relative grain boundary energy in the light of the information available from modern SEM diffraction techniques, i.e. when both the misorientation *and* the grain boundary plane orientation of boundaries in bulk materials are known.

2. Theoretical considerations.

2.1 THE INTERFACE-PLANE SCHEME FOR GRAIN BOUNDARY CHARACTERISATION.

— A simple measure of the change in orientation between two neighbouring grains provides the misorientation parameters necessary to apply a coincidence site lattice (CSL) categorisation to the boundary. The reciprocal density of coincidence sites is designated by Σ. If the inclination of the grain boundary plane is known, then the indices of the grain boundary surface with respect to both interfacing grains can be calculated. The experimental techniques involved are documented in detail elsewhere [7].

When the indices of the grain boundary have been measured, it is physically useful to describe the boundary geometry by these indices in both grain plus the twist angle between them. This is the 'interface-plane' scheme [12]. When the twist angle is zero the boundary is a tilt type. Two types of tilt boundaries are distinguished: symmetrical tilts, STBs, where the indices of the boundary plane are the same in both grains, and asymmetrical tilts, ATBs, where the indices are different. In the $\Sigma = 3$ system there are two STBs, namely the 111/111 'coherent twin' and the 211/211 'incoherent twin'. There are many ATBs in this system, e.g. 411/110.

2.2 GRAIN BOUNDARY FREE ENERGY AND DIHEDRAL ANGLES.

— Free energy is the central thermodynamic quantity which characterises grain boundaries, and boundaries will minimise their free energy where possible. In polycrystals the relative positions óf neighbouring grains are usually constrained such that mutual rotations are limited. For some specimen geometries, e.g. wires or thin sheets where grain boundaries traverse the full thickness of the specimen, grain-to-grain misorientation is restricted whereas grain boundary inclination (the angle between a boundary and the specimen surface) can change readily during annealing [13]. The torque which describes a couple acting on a grain boundary so as to rotate its inclination towards a lower energy is called the Herring torque [14].

Within bulk polycrystals grain boundaries are totally constrained by connectivity requirements such that torques cannot operate to any appreciable extent to minimise the free energy. A consequence of this constraint is that the relative free energies of three boundaries which share a common joining line form a triangle of forces under equilibrium conditions. This simple treatment of boundary energies as tensions which are 'pulled' along each boundary away from their common intersection, as shown in figure 1, leads to the well-known expression

$$\gamma_1/\sin \alpha_1 = \gamma_2/\sin \alpha_2 = \gamma_3/\sin \alpha_3 \tag{1}$$

where γ_j and α_j are the grain boundary free energies and dihedral angles respectively.

For a homogeneous boundary energy distribution the equilibrium configuration is a three grain junction with dihedral angles of 120°. However, in practice a distribution of dihedral angles is observed, implying inhomogeneous grain boundary energies [9-11, 15]. The most obvious example is that of an annealing twin ($\Sigma = 3$) boundary which is often observed to be associated with a dihedral angle of 180°. Equation (1) has frequently been used to estimate relative grain boundary
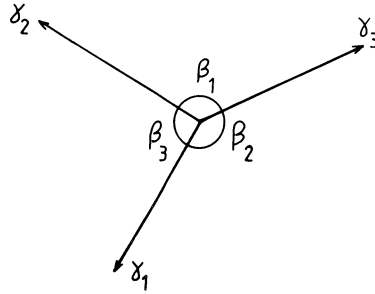
Fig. 1. — Schematic illustration of a planar section through three grain boundaries which have a common junction showing the distribution of boundary energies and dihedral angles. It is usually assumed that the boundary junction line is perpendicular to the plane of observation and that α, the true dihedral angle, is equivalent to β, the dihedral angle measured in the planar section.

energies from measurements of the dihedral angles on plane sections. Inherent in equation (1) are the assumptions that equilibrium has been reached i.e. the driving force for grain boundary migration is negligible, torque terms can be neglected and grain boundaries are planar and normal to the plane of observation.

The equilibrium of a junction where n grain boundaries meet is given by

$$[\gamma_j \, t_j + (t_j \times s) \, \partial\gamma_j/\partial\Phi_j] = 0 \qquad (2)$$

where γ_j is the grain boundary free energy, t_j are vectors in the boundary planes normal to the vector s which lies along the junction line of the boundaries, and the angles Φ_j characterise the boundary inclination with respect to the plane of observation. Usually, $n = 3$ unless low energy boundaries are present at the junction whereupon n can be > 3. $\partial\gamma_j/\partial\Phi_j$ is the Herring torque term. When the torque terms are negligible equation (2) reduces to equation (1) by substitution of $\cos\alpha_j$ for t_j.

Equation (1) refers to the *true* dihedral angles between boundary planes, although these are often taken to be equal to the *projected* dihedral angles as measured on the plane of observation (Fig. 2). There will only be equivalence between the true and projected dihedral angles when the common junction line of the boundaries, and thus the boundaries themselves, are perpendicular to the specimen surface. The true dihedral angles α_j can be obtained from a knowledge of the projected angles β_j and the angles of inclination of the component boundaries with respect to the specimen surface, Φ_j. Figure 3 shows on a stereogram the angular relationships between a three-grain junction where the junction line L is inclined with respect to the surface, as in figure 2. The relationship for spherical triangles can be applied to each of the three triangles bounded by the trace of two adjoining boundary planes and the trace of the specimen surface. In figure 2 the specimen surface coincides with the primitive of the stereogram. Solving spherical triangle ABL gives [10]

$$\cos\alpha_1 = -\cos\Phi_1 \cos\Phi_2 + \cos\beta_1 \sin\Phi_1 \sin\Phi_2 \qquad (3)$$

3. Experimental considerations.

3.1 COMPARISON BETWEEN TEM AND SEM FOR MEASURING GRAIN BOUNDARY PARAMETERS. — The crystallographic parameters and grain boundary inclination angle Φ can be obtained either
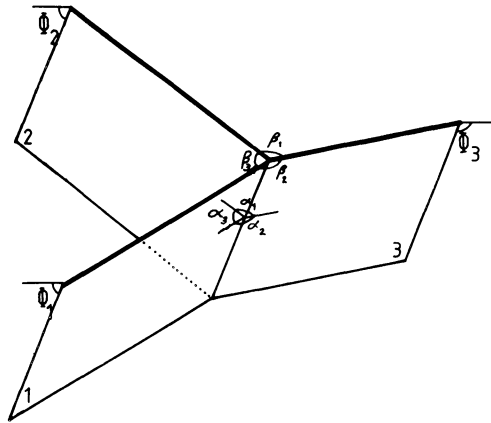
Fig. 2. — Schematic illustration of the three grain boundaries in figure 1, showing that the junction line is not perpendicular to the planar section, i.e. specimen surface, which is denoted by thick lines. Φ_1 Φ_2, Φ_3 are the inclinations of the respective boundaries, i.e. the angles between the specimen surface and the grain boundary.

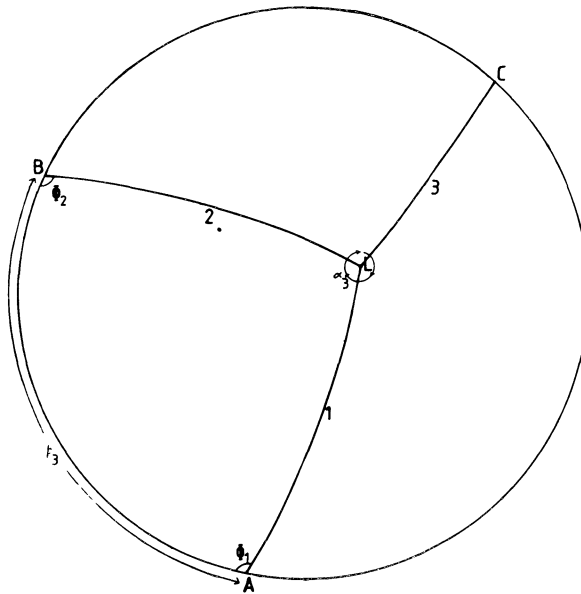Fig. 3. — Stereographic illustration of the grain boundaries and some of the parameters α_j, β_j and Φ_j from figure 2. L is the direction of the junction line.

from transmission electron microscopy (TEM) thin foil measurements or from calibrated serial sections of bulk specimens observed using scanning electron microscopy (SEM) [6, 7]. For TEM or sections parallel to the surface of bulk specimens Φ is given by

$$\tan \Phi = T/P \tag{4}$$

where T is either the foil thickness or the amount of bulk specimen removed by parallel sectioning, and P is either the projected boundary width for TEM or the displacement of the boundary/surface intersection before and after sectioning for SEM or optical microscopy. It is also possible to obtain Φ directly by a perpendicular sectioning method in the SEM [7, 17].

The SEM/EBSD route for obtaining grain boundary parameters has several advantages over that for TEM, namely
  – access to many grains (typically hundreds or thousands) per specimen;
  – easy specimen preparation;
  – semi-automatic or automatic orientation determination, which only a few TEMs have;
  – location of the sampled grains is known relative to the macroscopic specimen geometry;
  – grain boundary plane inclinations might be altered during TEM thin foil preparation;
  – calibrated serial sectioning can be carried out to obtain three-dimensional crystallographic information.

On the other hand, TEM allows access to fine structure imaging and analysis, e.g. dislocations, which is not possible with SEM.

3.2 EXPERIMENTAL PROCEDURES. — The dihedral angles of 105 grain boundary junctions in pure nickel, annealed under vacuum for 2 hours at 1000°C and having an average grain size of 170 μm, were measured. Boundary inclinations were obtained by a parallel serial sectioning method [7]. These were collated with the crystallographic geometry of each boundary as measured using electron backscatter diffraction in an SEM. For all boundaries the grain-to-grain misorientation was measured, and for more than two-thirds of the boundaries all five degrees of freedom were measured, i.e. both the misorientation and the orientation of the grain boundary surface with respect to each interfacing grain.

4. Results.

The crystallography of the grain boundaries in the sample population is as follows. Almost half (46%) of the analysed boundaries were $\Sigma = 3$s, and a further 10% were either $\Sigma = 9$s or $\Sigma = 27$s. Almost all the $\Sigma = 3$ category were either the 111/111 symmetrical tilt boundary (STB) or, more frequently, asymmetrical tilt boundaries (ATBs).

The distribution of grain boundary inclinations is shown in figure 4 which indicates that the majority of boundaries (70%) are nearly perpendicular (within 20°) to the specimen surface. It is also shown in figure 4 that the angle of inclination correlates with increasing $\Sigma = 3$ proportions. The present data show a strong trend for boundaries to align nearly perpendicular to the specimen surface because during annealing these boundaries have some rotational freedom and can lower their energy by area minimisation (i.e. aligning perpendicular to the specimen surface). This can be contrasted to a 'non-surface' population of boundaries in 304 stainless steel where the frequency distribution of boundary inclinations is much flatter [10].

Since most of the boundaries were nearly perpendicular to the specimen surface, the projected dihedral angles were within a few degrees of the true angles. For example at a junction where the boundary inclinations and projected dihedral angles were 70°, 70°, −84°, and 131°, 123°, 106° respectively, the true dihedral angles were 125°, 123°, 111°. Figure 5 shows the distribution of dihedral angles for three-grain junctions, compiled separately for junctions including or not including $\Sigma = 3$s. The two distributions are markedly different: the $\Sigma = 3$ distribution is skewed to both high and low dihedral angles whereas that for non− $\Sigma = 3$s is normally distributed. The mean and standard deviation for the non− $\Sigma = 3$ distribution is 120.02° and 20.7° respectively. All the grain junctions except five comprised three grains. Of these five junctions, four comprised
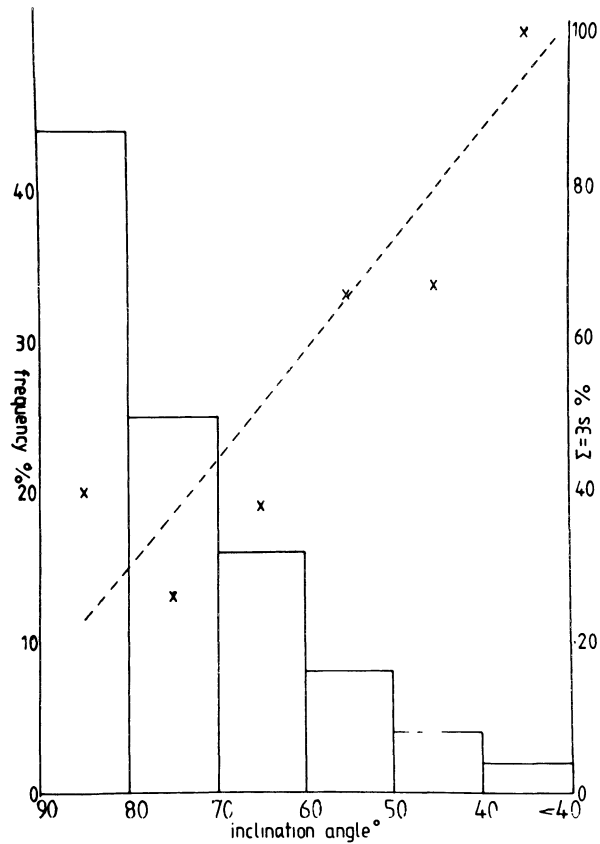
Fig. 4. — Frequency distribution of grain boundary inclinations for the whole sample population. The proportion of $\Sigma = 3$s in each group is marked; smaller inclination angles correlate with higher proportions of $\Sigma = 3$s.

four grains and one five grains, all involving $\Sigma = 3^n$ boundaries where $n = 1$ to 4 [1]. Junctions of four boundaries are stable if at least one of them has a low energy.

The distribution of non– $\Sigma = 3$ boundaries is very similar to that reported for austenitic steel [10], and the standard deviation agrees generally with data from NiMn2 [9]. The large dihedral angles associated with $\Sigma = 3$s has been noted on many previous occasions. However, more detailed interpretation of the data is possible here since for many of these all five degrees of freedom, i.e. grain boundary planes plus the twist angle between them, have been measured. Four classes of $\Sigma = 3$ boundaries, based on the indices of their planes, were identified:

  a) 111/111 STBs;

  b) ATBs on the 011 zone;

  c) ATBs on zones other than the 011 zone;

  d) 'General' $\Sigma = 3$ boundaries.

The significance of separating $\Sigma = 3$s on the 011 zone (e.g. 411/110 or 311/771 ATBs) from other ATBs is that computer simulations have shown that the former lie in an energy valley [16]. Figure 6 shows the distribution of dihedral angles associated with $\Sigma = 3$ boundaries for those cases where the boundary plane had been measured and classified according to one of the four groups above. The trend which emerges is that the dihedral angle of most STBs and ATBs is 175-
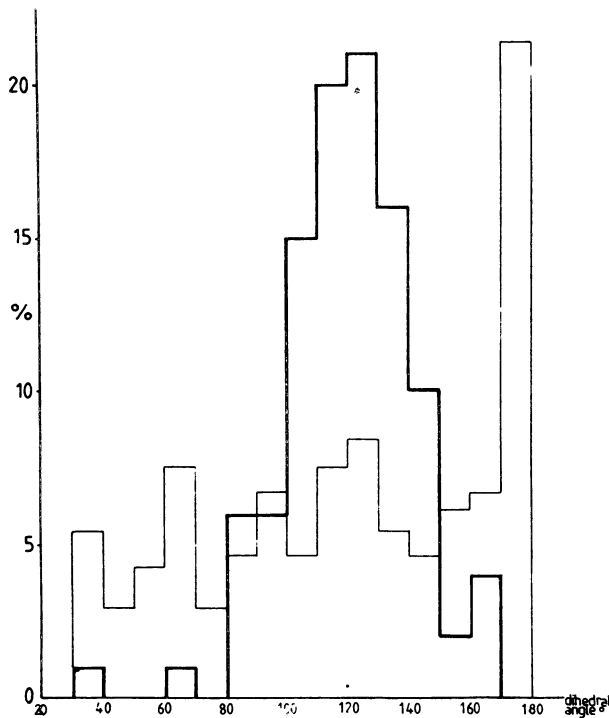
Fig. 5. — Frequency distribution of dihedral angles for three-grain junctions which have one or more $\Sigma = 3$ boundaries (light line) and three-grain junctions which do not have $\Sigma = 3$ boundaries (heavy line).

180° whereas that of the general $\Sigma = 3$s is smaller. Although this result indicates that $\Sigma = 3$s which are tilt boundaries have lower energies than $\Sigma = 3$s with irrational boundary planes, the majority of $\Sigma = 3$s have dihedral angles which approach 180° even through boundaries of varying energy will fall within this category. For example, the energy of 111/111 STBs is known to be lower than that of any ATBs, yet the resolution of the dihedral angle method for determining relative boundary energies is insufficient to distinguish them.

The data from the $\Sigma = 3$ set highlights the fact that the dihedral angle method of estimating grain boundary energy provides only *relative* boundary energies at each grain junction. The angle will therefore depend, amongst other factors, on the energy of each boundary at a grain junction. If equation (1) applies, a boundary with a dihedral angle of 175-180° has an energy which is one to two orders of magnitude less that of a random high angle boundary. Furthermore other factors may influence the dihedral angles distribution as discussed in the next section.

Low angle and $\Sigma = 9$ boundaries are categorised in the non− $\Sigma = 3$ data set unless they are associated with $\Sigma = 3$ boundaries at a grain junction. However table I shows that low angle or $\Sigma = 9$ boundaries are associated with dihedral angles >120° when $\Sigma = 3$s are not present at the same grain junction. These dihedral angles contribute to the broadening of the upper end of the distribution for the non− $\Sigma = 3$ histogram in figure 5. The implication of these results is that the energy of $\Sigma = 9$ and these low angle boundaries is lower than of an average boundary. The grain boundary planes of $\Sigma = 9$ types, where they could be measured, were 411/110, 410/410 and 511/111.
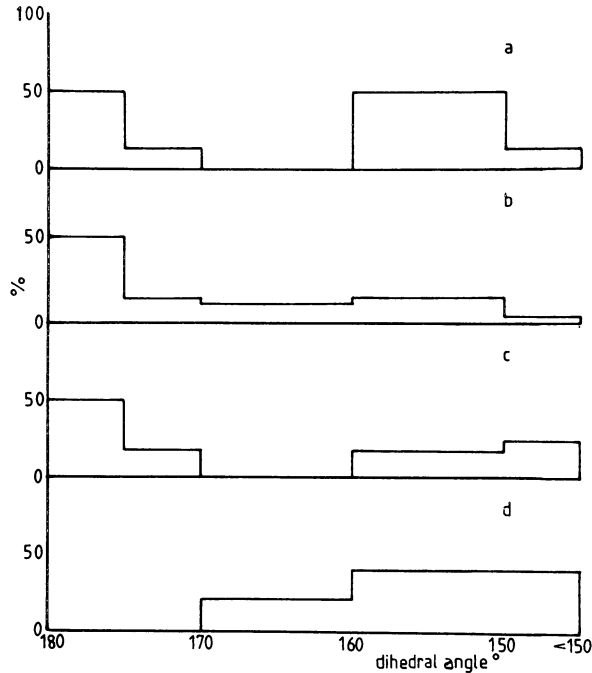
Fig. 6. — Frequency distribution of dihedral angle for $\Sigma = 3$ boundaries whose plane indices have been determined. a) 111/111 STBs; b) ATBs on the $0\bar{1}1$ zone; c) other ATBs; d) $\Sigma = 3s$ with general boundary planes.

Table I. — *Dihedral angles for $\Sigma = 9$ and low angle boundaries (L) ($\Sigma = 3$ boundaries not present at the same grain junction).*

Boundary	Dihedral angle °	Plane indices
9	144	111/511
9	147	110/411
9	135	410/410
9	160	—
L	142	—
L	140	—

5. Discussion.

The principal finding of this work is the distribution of grain boundary plane indices for $\Sigma = 3$ and $\Sigma = 9$ boundaries in nickel (mostly tilts) and the accompanying distribution of dihedral angles (which from equation (1) gives the relative energies) for these particular boundaries. Some aspects of the application of equation (1) to the present grain boundary geometrical data will now be discussed.

The central tenet of the relationship between grain boundary free energy and dihedral angle is that the triangle of forces is in equilibrium. True equilibrium will exist when the driving force for

grain boundary migration and/or rotation is negligible. Prior to this, metastable equilibrium will exist when some boundaries are in energy 'cusps', that is, they have achieved energies which are local minima but not necessarily among the lowest energy boundaries in absolute terms. This is the case for many of the $\Sigma = 3$ boundaries reported here. With further annealing, the dihedral angles may be modified.

There is experimental evidence that the distribution of grain boundary inclinations for those boundaries which join a free surface is different to that of boundaries in the bulk of polycrys-tals [18], especially after those boundaries which join the free surface are annealed. The surface boundaries clearly have more rotational freedom than those in the bulk of the material. It is possi-ble that some grain rotation occurs, but more typically the grain boundaries themselves will rotate under the Herring torque into positions of metastable equilibrium. Figure 4 shows evidence for this since non-$\Sigma = 3$ boundaries have tended to align perpendicular to the specimen surface, which lowers their free energy by specific area minimisation. On the other hand figure 4 also shows that a lower energy may be achieved for $\Sigma = 3$ boundaries by adopting a tilt configuration rather than the minimum area criterion. These trends are more polarised for specimens where grain boundaries traverse corners, and this work is described elsewhere [17].

Clearly for specimens where annealed grain boundaries abut the surface it is an approxima-tion to neglect torque terms, although for grain boundaries in the bulk it is probably acceptable since these have limited rotational freedom. Previous work has shown that the magnitude of the normalised Herring torque, $1/\gamma \, \partial\gamma/\partial\Phi$, is $> 0.03 \deg^{-1}$ for coherent twins and an order of magni-tude smaller for random high angle boundaries [13]. The present work indicates that the Herring torque has operated to rotate many of the random high angle boundaries towards the minimum area position and convesely to rotate planes of $\Sigma = 3$s into crystallographic configurations as-sociated with energy cusps. These configurations do not, in general, coincide with the minimum area position. Consequently, equation (2) should be used to estimate grain boundary energies where low energy boundaries such as some $\Sigma = 3$ types are involved and equation (1) can be used only qualitatively. Omission of the torque term, i.e. applying equation (1) when torques have influenced the boundaries in question, leads to overestimated energies.

Even for well annealed specimens where grain boundary curvature has largely been removed by grain growth a boundary may not be planar over its entire surface. However, a boundary has a double curvature and the appearance of a straight boundary trace on the specimen surface is usually taken to indicate a planar boundary. With regard to the true dihedral angles, it has been shown that for the present work the majority of boundaries are within 20° of being perpendicular to the surface, and that only a small error is involved if projected rather than the true dihedral angles are used in equation (1). Furthermore, it has been established that for 'surface' grain boundaries only a qualitative estimate of the boundary energy can be made, and for these cases it is clear that measurement of projected dihedral angles is sufficient.

6. Concluding remarks.

For measurement of grain boundary crystallography — grain misorientations and grain boundary plane geometry — EBSD in the SEM has several advantages over the TEM. The former technique has been used to generate a data set of grain boundary plane geometries plus dihedral angles in nickel. $\Sigma = 3$ boundaries were widespread, with the majority of them being either symmetrical or asymmetrical tilts. An analysis of dihedral angles associated with $\Sigma = 3$ boundaries revealed that both symmetrical *and* asymmetrical tilts were associated with dihedral angles which approach 180° whereas other $\Sigma = 3$s (general boundary planes) were associated with smaller dihedral angles. From this it is inferred that many asymmetrical tilt boundaries in nickel have very low

energies compared with random boundaries. The resolution of the dihedral angle measurement technique was insufficient to distinguish a hierarchy of energies within the $\Sigma = 3$ tilt class. At grain junctions where a $\Sigma = 9$ boundary or a low angle boundary was present, but not a $\Sigma = 3$, these boundaries were associated with a large dihedral angle. Other CSLs were not. Thus $\Sigma = 9$ and low angle boundaries in nickel have lower than average energies.

Acknowledgements.

References

[1] RANDLE V., *Acta. Met. Mat.* (overview) (1993) in press.
[2] RANDLE V., Microtexture Determination and its Applications (Institute of Materials, London, 1993).
[3] DINGLEY D.J. and RANDLE V., *J. Mat. Sci.* **27** (1992) 4545-4566.
[4] BOLLMANN W., *Philos. Mag. A* **57** (1988) 637-649.
[5] RANDLE V., *Scrip. Met. Mat.* **28** (1993) 889-893.
[6] RANDLE V., *Mat. Sci. Tech.* **7** (1991) 985-990.
[7] RANDLE V., Grain Boundary Geometry in Cubic Polycrystals, (Institute of Physics Publishing, Bristol, U.K.).
[8] RHINES F.N., *Met. Trans.* **1** (1970) 1105-1120.
[9] KURZYDLOWSKI K.J., *Mat. Charac.* **26** (1991) 57-60.
[10] MURR L.E., *J. Appl. Phys.* **39** (1968) 5557-5566.
[11] MURR L.E., SMITH P.J. and GILMORE G.M., *Philos. Mag.* **17** (1968) 89-106.
[12] WOLF D. and LUTSKO J.F., *Zeit. Kristall.* **189** (1989) 239-262.
[13] OMAR R., PhD. Thesis (University of Warwick, U.K., 1987).
[14] HERRING C., The Physics of Powder Metallurgy, W.E. Kingston Ed. (McGraw Hill, New York, 1951) 143-150.
[15] KURZYDLOWSKI K.J. and PRZETAKIEWICZ W., *Scri. Metall.* **22** (1988) 299-300.
[16] WOLF U., ERNST F., MUSCHIK T., FINNIS M.W. and FISCHMEISTER H.F., *Philos. Mag. A* **66** (1992) 991-1016.
[17] RANDLE V. and DINGLEY D.J., *Scr. Metall.* **23** (1989) 1565-1570.
[18] HULL F.C., *Mat. Sci. Tech.* **4** (1988) 778-785.